

An exactly solvable model for Dynamic Nuclear polarization

Inés Rodríguez-Arias,¹ Markus Müller,^{2,3} Alberto Rosso,¹ and Andrea De Luca⁴

¹*LPTMS, CNRS, Univ. Paris-Sud, Université Paris-Saclay, 91405 Orsay, France*

²*Condensed matter theory, Paul Scherrer Institute, CH-5232 Villigen PSI, Switzerland*

³*The Abdus Salam International Centre for Theoretical Physics, 34151, Trieste, Italy*

⁴*The Rudolf Peierls Centre for Theoretical Physics,
Oxford University, Oxford, OX1 3NP, United Kingdom*

We introduce a solvable model which elucidates the role of Anderson localization in driven disordered magnets, as used in the context of dynamic nuclear polarization. Instead of spins, we study a set of non-interacting fermions that are coupled locally to nuclear spins and tend to hyperpolarize them. The induced hyperpolarization is a fingerprint of the state of the fermions, which undergo an Anderson Localization (AL) transition upon increasing the disorder. Our central result is that the maximal hyperpolarization level is found close to the localization transition, which we explain by the evolution of correlations among overlapping fermionic levels in the vicinity of criticality.

I. INTRODUCTION

Statistical mechanics is grounded on the assumption that simple macroscopic laws emerge whenever time evolution is so complex that specific details become irrelevant. Although this picture is generically confirmed in the evolution of closed quantum system, recent progresses¹ have predicted that the presence of strong disorder can prevent thermal equilibrium to be reached when a quantum system evolves under its own dynamics. This phenomenon occurs a sharp transition and goes under the name of many-body localization (MBL). Direct confirmations of MBL have been obtained in highly controlled experimental settings, as ultra-cold atomic fermions^{2,3}, and chains of trapped ions⁴. On the other hand, most of the theoretical studies focused on isolated one-dimensional lattice systems where the main features of MBL phase have been well characterized^{5–12}.

However, a small coupling with environment is present in any physical system, even in cold-atoms and trapped ions. Moreover, standard solid state systems will always feel the presence of the bath of phonons on sufficiently long time scales. For these reasons, recent studies have started to address the fate of the MBL transition in the presence of weak dissipation^{13–15}. In particular, at sufficiently long times, the presence of the environment always restores ergodicity in an otherwise localized phase. Nevertheless, when a weakly dissipative system is driven out-of-equilibrium, it can reach a stationary state whose characteristics will strongly depend on whether its intrinsic dynamics is ergodic or non-ergodic - even though, in general, no genuine transition, but only a strong crossover, survives in the space of steady states. To date, mainly two experimental settings of driven dissipative systems have been studied in this context: interacting gases of Rydberg atoms¹⁶ and dynamic nuclear polarization (DNP) protocols^{17–19}. Here we focus on the latter, for which it has been shown that the MBL transition of the closed system manifests itself in key features of the driven system.

DNP is a very promising technique to cool nuclear

spins and thereby improve the signal-to-noise ratio in nuclear magnetic resonance (NMR) measurements. The procedure is as follows: a glassy sample of the nuclear compound is doped with radicals, i.e., molecules with unpaired electron spins. The sample is then cooled down to temperature of the order of 1 K and subjected to a strong magnetic field B , which in many standard experiments is fixed to $B = 3.35T$. Under these conditions, electron spins have a high polarization level, whereas nuclear spins remain almost unpolarized and thus yield a very small NMR signal. The sample is then driven out of equilibrium by a microwave field. By tuning the frequency of the microwaves close to the Zeeman gap of the electron spins, one observes a huge transfer of polarization from the electron spin system to the nuclear spin system, which results in strongly enhanced NMR contrast. It is thus paramount to understand the underlying cooling mechanism so as to be able to optimize the resulting cooling of the nuclear spins.

In a recent work¹⁸, we showed that the efficiency of the procedure (i.e., the final nuclear polarization) depends on the interplay between the disorder arising from the g -factor anisotropy of the electron spins, and their dipolar interactions, whose magnitude is controlled by the radical concentration. For strong interactions, the electron spins are ergodic, and their stationary state can be described by an effective spin-temperature^{20,21}. In contrast, when disorder is dominant and the closed system is localized, the stationary nuclear polarization was found to rapidly drop. As a consequence, the optimal value is attained close to the MBL transition.

This results were obtained by exactly diagonalizing an interacting electron system, which however was limited to small system sizes with up to 13 spins. That study did however not furnish a thorough understanding of the crossover from the ergodic into the localized regime, and the associated maximum in the cooling effect. In order to go beyond these limitations, in this paper, we present the study of a free-fermion analogue of the electron spin problem, which allows treating much larger sizes ($\simeq 10^4$). Because of integrability, free fermions do not present a genuine ergodic phase. Nevertheless, disorder tunes a

(single-particle) localization transition, which we find to result in the same essential features of the driven steady state as in the many-body spin system; in particular, the maximal nuclear polarization is reached when the electrons are close to the localization transition. Our toy model has the crucial advantage that the properties of this crossover are much more accessible to analytical insight. Indeed, the stationary nuclear polarization is put in direct relation to basic quantities such as the inverse participation ratio and the eigenfunction correlation, which describe the critical behavior of the Anderson transition.

II. MICROSCOPIC DESCRIPTION OF DNP

The full Hamiltonian describing the DNP protocol accounts for two spin species: nuclear and electronic. Intra-species interactions are given by the dipolar couplings, while nuclear and electron spins are coupled predominantly through hyperfine interactions. The Hamiltonian of the isolated spin system can thus be written as the sum of three terms:

$$\hat{H}_s = \hat{H}_e + \hat{H}_n + \hat{H}_{e-n}, \quad (1)$$

where the first and second terms stand, respectively, for the electronic and nuclear subsystems and the last term takes into account the hyperfine interactions. Let us describe each term more in detail:

$$\hat{H}_e = \sum_{j=1}^{N_e} \omega_j \hat{S}_j^z + \hat{H}_e^{(dip)}, \quad \hat{H}_{e-n} = \sum_{j=1}^{N_e} A_j \hat{S}_j^z \hat{I}_j^x, \quad (2a)$$

$$\hat{H}_n = -\omega_n \sum_{p=1}^{N_n} \hat{I}_p^z + \hat{H}_n^{(dip)}, \quad (2b)$$

where \hat{S}_j^ℓ and \hat{I}_p^ℓ are respectively the ℓ -component of the electron and nuclear spin operators and N_e, N_n their numbers. The Larmor frequencies ω_j and ω_n result from the external magnetic field. Electron spins display inhomogeneities in the Larmor frequencies, i.e. $\omega_j = \omega_e + \delta\omega_j$, due to the local g -factor anisotropy, which are instead negligible for the nuclear spins. The coefficients A_j indicate the strength of hyperfine interactions: here, we assume that, among the N_n nuclear spins, only N_e are *core* nuclear spins, i.e. with a significative interactions with electron spins. For the sake of simplicity, each core nuclei is attached to one electron spin. We use \hat{I}_j^ℓ to label those spins and \hat{I}_p^ℓ to label the full set of spins. The exact form of the dipolar Hamiltonians $\hat{H}_{e/n}^{(dip)}$ is given in Appendix A.

Moreover, the system is weakly coupled to a reservoir at a temperature β^{-1} and irradiated by a microwave field of frequency ω_{MW} that couples with an amplitude ω_1 to the electron spins. All in all, the full Hamiltonian of the

system reads :

$$\hat{H}_{total} = \hat{H}_e + \hat{H}_n + \hat{H}_{e-n} + \hat{H}_R + \hat{H}_{S-R} + \hat{H}_{MW}, \quad (3)$$

with the microwave Hamiltonian $\hat{H}_{MW} = \omega_1 \sum_j \hat{S}_j^x \cos(\omega_{MW}t)$. The term \hat{H}_R governs the dynamics of the reservoir and \hat{H}_{S-R} contains the coupling of the spin system with the reservoir. Describing exactly this system would be a formidable task and one is forced to resort to some approximations.

A. Review of Lindblad approximation schemes

A possible way-out is to treat separately fast and slow time-scales in the total system: $\hat{H}_{total} = \hat{H}_{fast} + \hat{H}_{slow}$. This allows performing the weak-coupling approximation, leading to an equation for the density matrix of the spin system in a Lindblad form²²: the unitary dynamics due to \hat{H}_{fast} is treated exactly, while the contribution of \hat{H}_{slow} is taken into account perturbatively. Consistently with this approximation, one can obtain a further simplification projecting the Lindblad equation onto the eigenstates of \hat{H}_{fast} . In this way, the dynamics reduces to a master equation describing the probability of occupying an eigenstate $|n\rangle$ of \hat{H}_{fast} : \hat{H}_{slow} only determines the transition rates between pairs of eigenstates $|n\rangle, |m\rangle$ through matrix elements of all the local operators \hat{O} involved in \hat{H}_{slow} , i.e. $|\langle n|\hat{O}|m\rangle|^2$. Within this approach, to take into account the time-dependent microwaves, one resorts to the rotating-wave approximation²¹, which amounts to neglecting fast oscillating terms and thereby obtaining a static Hamiltonian in the rotating frame.

Different schemes are obtained according to how \hat{H}_{total} is split into \hat{H}_{fast} and \hat{H}_{slow} . Given that the coupling with the reservoir and microwaves is always weak, a first possibility, discussed in [23,24,18], is to include in \hat{H}_{slow} the last three terms of (3). Although this is a huge simplification of the original problem, one has to face the non-trivial task of diagonalizing the interacting Hamiltonian in (1) and computing the appropriate matrix elements between its eigenstates. In absence of further simplifications, one is limited to the use of exact diagonalization and small system sizes (maximum of 20 electron spins). This was the route followed in [18].

A second approach, proposed in [25,26], consists in including in \hat{H}_{slow} not only the coupling with the reservoir and microwave, but also all the interaction terms inside \hat{H}_s . In this way, the eigenstates $|n\rangle$ become simply product states in the direction of the magnetic field and the rates can be computed analytically. The solution of the master equation can be obtained with Monte Carlo for much larger system sizes. However, in order for this approach to be efficient, all the rates have to be of the same order of magnitude: this was successfully used in [25,26] in the presence of a single electron spin to model the process of nuclear spin diffusion. Instead, when many electron spins are considered, the presence

of inhomogeneities and their fast dynamics render this method inefficient.

III. A NEW APPROACH

Here, we propose a different approach that allows dealing with a large number of electrons (N_e up to 10^4). We treat perturbatively the hyperfine interaction \hat{H}_{e-n} , so that the eigenstates of the whole spin system factorize as

$$|n\rangle = |A\rangle \otimes |\mu\rangle \quad (4)$$

with $|A\rangle$ an eigenstate of \hat{H}_n and $|\mu\rangle$ one of \hat{H}_e . For the nuclear system, given the absence of any inhomogeneities and the smallness of their dipolar interaction, we focused on two extremal limit: i) a single nuclear spin; ii) a perfectly ergodic many-body system of nuclear spins which satisfies the eigenstate thermalization hypothesis (ETH). Given the fast nuclear spin diffusion compared to other nuclear processes, the latter is the most relevant for experimental applications. For the electron spins, in order to take into account the competition between dipolar interaction and inhomogeneities, we resort to a strong simplification.

A. Electron spins as a free-fermion model

Let us replace the spin degrees of freedom with fermionic ones

$$\hat{S}_j^x \rightarrow \frac{\hat{c}_j^\dagger + \hat{c}_j}{2}, \quad \hat{S}_j^y \rightarrow -i \frac{\hat{c}_j^\dagger - \hat{c}_j}{2}, \quad \hat{S}_j^z \rightarrow \frac{1}{2} - \hat{c}_j^\dagger \hat{c}_j. \quad (5)$$

so that a value of $\hat{S}_j^z = \pm 1/2$ corresponds to an empty or occupied site j , respectively. The fermionic operators satisfy the anti-commutation relation $\{\hat{c}_i^\dagger, \hat{c}_j\} = \delta_{ij}$. For a single-site j , this is an exact mapping, as it correctly reproduces all the spin commutation relations. However, for different sites, spins commute while fermions anti-commute. In 1D, this problem can be handled including a non-local contribution to Eq. (5), according to the Jordan-Wigner recipe. However, in higher dimensions, while the introduction of meandering JW tails is still possible, such an exact mapping becomes impracticable and one is forced to make some approximations. Here, we start from the substitutions (5) in (2a), which we further simplify to obtain an exactly solvable tight-binding hopping model that we nevertheless expect to reproduce essential features of the DNP phenomenology, especially to capture the transition from the localized to the delocalized phase (see Appendix A for a detailed discussion):

$$\hat{H}_A = \sum_i \Delta_i \hat{c}_i^\dagger \hat{c}_i - t \sum_{\langle i,j \rangle} \left(\hat{c}_i^\dagger \hat{c}_j + \hat{c}_j^\dagger \hat{c}_i \right) + \omega_e \sum_i \hat{c}_i^\dagger \hat{c}_i, \quad (6)$$

where the Δ_i are uniformly distributed in the interval $[-w/2, w/2]$. The hopping parameter t between nearest neighbours parameterizes the strength of dipolar interaction, as for instance, after our replacement (5) $\hat{S}_j^+ \hat{S}_k^- \rightarrow \hat{c}_j^\dagger \hat{c}_k$. In standard DNP condition for trityl radical, the external magnetic field of $B = 3.35$ T is responsible for the chemical potential term with $\omega_e = 93.9$ (2πGHz) and, via the g-factor anisotropy, for the strength of the disorder $w = 108$ (2πMHz). This Hamiltonian corresponds to the 3D-Anderson model and the advantage of this model is that it combines integrability with the presence of a localization transition at a critical value of the ratio between disorder and hopping, which for a cubic array of sites and box-distributed disorder takes the value $w/t = (16.536 \pm 0.007)$ [27].

To solve this model, one introduces new fermionic operators $a_\alpha = \sum_i \phi_{\alpha i}^* \hat{c}_i$, or equivalently $\hat{c}_i = \sum_\alpha \phi_{\alpha i} a_\alpha$. The coefficients $\phi_{\alpha i}$ describe the single-particle wavefunction that corresponds to the eigenvector of the matrix

$$M_{ij} = \begin{cases} \omega_i & i = j \\ -t & i, j \text{ nearest neighbours} \end{cases} \quad (7)$$

with eigenvalue ϵ_α and verify the orthogonality and completeness relations, i.e., $\sum_i \phi_{\alpha i}^* \phi_{\beta i} = \delta_{\alpha\beta}$ and $\sum_\alpha \phi_{\alpha i}^* \phi_{\alpha j} = \delta_{ij}$. In terms of $a_\alpha, a_\beta^\dagger$, one obtains the diagonal Hamiltonian

$$\hat{H}_A = \sum_{\alpha=1}^{N_e} \epsilon_\alpha a_\alpha^\dagger a_\alpha, \quad (8)$$

The many-body eigenstates of (8) can be written as

$$|\mu\rangle = |n_1^\mu, n_2^\mu, \dots, n_{N_e}^\mu\rangle = \prod_{\alpha=1}^{N_e} (a_\alpha^\dagger)^{n_\alpha^\mu} |0\rangle, \quad (9)$$

where $n_\alpha^\mu \in \{0, 1\}$ is the occupation number of the mode α in the many-body eigenstate $|\mu\rangle$. Their energy is given as $E_\mu = \sum_\alpha n_\alpha^\mu \epsilon_\alpha$. This is a huge simplification as compared to the original spin problem, since determining the many-body eigenstates of \hat{H}_A only requires the numerical diagonalization of the matrix M_{ij} in (7), whose size grows linearly with the volume of the system.

In our simulations, we consider a cubic lattice of linear size L , corresponding to $N_e = L^3$ spins in the original model. Then, the Anderson transition occurs at $t_c \approx (6.6 \pm 0.2)$ (2πMHz). In figure 1, the density of states (DOS) $\rho(\epsilon) = N_e^{-1} \sum_\alpha \delta(\epsilon - \epsilon_\alpha)$ is shown for different values of t : this is a self-averaging quantity which is not affected by the localization transition; for large t , its shape is enlarged and smoothed out from the box distribution in absence of hopping.

B. Relaxation and microwave dynamics in the free-fermion model

The free fermions are driven to an out-of-equilibrium stationary state by the microwave irradiation and kept in contact with the thermal bath at a temperature β^{-1} . Both bath and microwaves induce electron spin flips which cause transitions between two eigenstates of the spin system $|n\rangle$ and $|m\rangle$. The general expressions for the corresponding rates were derived in [18, 17]. In our fermionic model, spin flip in a site j correspond to creation/annihilation of a fermion at such site. Thanks to the factorization in (4), the nuclear state $|A\rangle$ in these processes will be unchanged and using (9), one arrives (see appendix B 1) to:

$$W_{\mu \rightarrow \nu}^{\text{BATH}} = \sum_{\alpha} \frac{h(\Delta E_{\mu\nu})}{T_{1e}} |\langle \mu | (a_{\alpha}^{\dagger} + a_{\alpha}) | \nu \rangle|^2, \quad (10a)$$

$$W_{\mu \rightarrow \nu}^{\text{MW}} = \sum_{\alpha} \frac{T_{2e} \omega_1^2 |\langle \mu | (a_{\alpha}^{\dagger} + a_{\alpha}) | \nu \rangle|^2}{1 + T_{2e}^2 (|\Delta E_{\mu\nu}| - \omega_{\text{MW}})^2}. \quad (10b)$$

Here, the function $h(\epsilon) = e^{\beta\epsilon}/(1 + e^{\beta\epsilon})$ assures the detailed balance characteristic of a thermal equilibrium at temperature β^{-1} ; T_{1e} and T_{2e} are respectively the relaxation and coherence times for the electron spins system and $\Delta E_{\mu\nu} = E_{\mu} - E_{\nu}$. Note that in order for these rates to be non vanishing, the states $|\mu\rangle$ and $|\nu\rangle$ must differ in only one single mode occupation n_{α} . Therefore, only the single-particle energies ϵ_{α} are required, to obtain explicitly the rates in (10). As a consequence, in absence of the hyperfine couplings, different single-particle modes α decouple. Defining as $\hat{n}_{\alpha} = a_{\alpha}^{\dagger} a_{\alpha}$ the occupation number operator for the mode α , we can obtain its stationary expectation value as $\langle \hat{n}_{\alpha} \rangle_{t \rightarrow \infty} = (1 + P_B(\epsilon_{\alpha}))/2$, with

$$P_B(\epsilon) = \frac{[1 + T_{2e}^2(\epsilon - \omega_{\text{MW}})^2] \times \tanh(\beta\epsilon/2)}{1 + T_{2e}^2(\epsilon - \omega_{\text{MW}})^2 + 2\omega_1^2 T_{1e} T_{2e}}. \quad (11)$$

This expression coincides with the stationary polarization of a single-spin coupled to a bath and in presence of microwave irradiation, namely the Bloch equation. From these quantities one can obtain the expression for the stationary occupation probability of any eigenstate $|\mu\rangle$

$$p_{\mu}^{\text{stat}} = \frac{1}{2^{N_e}} \prod_{k=1}^{N_e} [1 - (-1)^{n_{\alpha}^{\mu}} P_B(\epsilon_{\alpha})] \quad (12)$$

C. Rates involving nuclear transitions

The hyperfine interactions \hat{H}_{e-n} in (2a) induces two types of transitions (see appendix B 2 for the details):

a. A three-spin transition labelled *ISS* which is responsible for the *cross-effect* mechanism of hyperpolarization. This transition involves the spin-flip of a nuclear

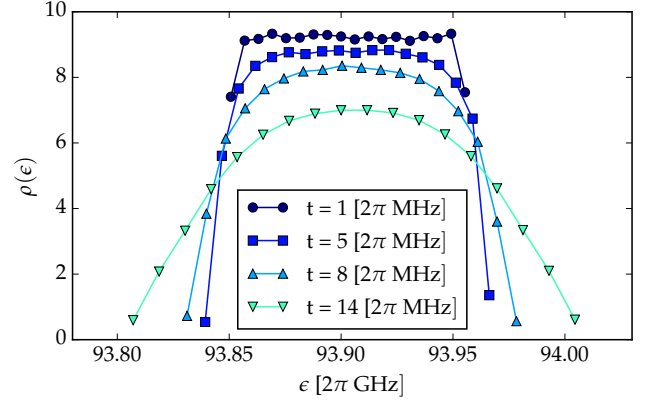


FIG. 1. Density of states of the 3D-Anderson Model for a system of linear size of $L = 8$ for different values of the hopping parameter $t = 2.2, 6.2, 10.2, 14.2$ (2πMHz) in inverted and regular triangles, squares and dots respectively.

spin together with the *flip-flop* of two electron spins. In our free-fermion model, the flip-flop transition can connect eigenstates $|\mu\rangle$ and $|\nu\rangle$ only if they differ in the occupation number of two single-particle modes, as in the example:

$$|A\rangle \times |0, \underbrace{1}_{\alpha}, 1, \underbrace{0}_{\beta}\rangle \rightleftharpoons |B\rangle \times |0, \underbrace{0}_{\alpha}, 1, \underbrace{1}_{\beta}\rangle, \quad (13)$$

where $|A\rangle$ and $|B\rangle$ are two eigenstates of \hat{H}_n , whose features will be specified later. The rate of the process in (13) involving the spin-flip of the nucleus j is

$$W^{\text{ISS}} = \frac{T_{2n} A_j^2 |\phi_{\alpha,j}|^2 |\phi_{\beta,j}|^2 |\langle A | \hat{I}_j^x | B \rangle|^2}{1 + T_{2n}^2 (|\epsilon_{\alpha} - \epsilon_{\beta}| - \omega_n)^2}, \quad (14)$$

where T_{2n} indicates the coherence time of a nuclear spin. Clearly, it becomes very efficient when the resonance condition $|\epsilon_{\alpha} - \epsilon_{\beta}| \sim \omega_n$ is matched.

b. A *polarization-loss* (PL) transition where a nuclear spin flip leaves the many-body fermionic state unchanged, as in the following example:

$$|A\rangle \times |\mu\rangle \rightleftharpoons |B\rangle \times |\mu\rangle \quad (15)$$

for any fermionic eigenstate $|\mu\rangle$. The rate of the process in (15) induced by the operator \hat{I}_j^x writes:

$$W^{\text{PL}} = \frac{T_{2n} A_j^2 |\langle A | \hat{I}_j^x | B \rangle|^2}{1 + T_{2n}^2 \omega_n^2} \left[\sum_{\alpha} |\phi_{\alpha,j}|^2 (n_{\alpha}^{\mu} - \frac{1}{2}) \right]^2. \quad (16)$$

Note that this term is always off-resonance and therefore its effect is rather weak as compared to the other transitions. In particular, dissipative processes that decrease nuclear polarization are governed by the contact with the

bath, which induces the leakage rate

$$W_{A \rightarrow B}^{\text{LEAK}} = \sum_{p=1}^{N_n} \frac{h(\Delta E_{AB})}{T_{1n}} |\langle A | \hat{I}_p^x | B \rangle|^2. \quad (17)$$

with $h(x)$ defined below Eqs. (10) and T_{1n} the relaxation time of a nuclear spin due to contact with the bath. These processes are typically more relevant than W^{PL} , as they involve all the nuclei and not only those coupled to electrons.

IV. COMPUTING THE NUCLEAR POLARIZATION

Equations (10), (14), (16) and (17) define the rate equations governing the occupation of the many-body eigenstates of the free fermion model which mimicks the spin system. The stationary state is given by the occupation probabilities p_n^{stat} , obtained as the eigenvector associated to the vanishing eigenvalue of the *transition matrix*

$$T_{n,n'} = W_{n' \rightarrow n}^{\text{tot}} - \delta_{n,n'} \sum_m W_{n \rightarrow m}^{\text{tot}}, \quad (18)$$

where $W_{n' \rightarrow n}^{\text{tot}}$ is the sum of all rates for processes from $|n\rangle$ to $|n'\rangle$. The size of this matrix is huge, as it scales as $2^{N_e + N_n}$. However, the simple structure of many-body eigenstates based on the factorization (4) and on the free-fermion approximation allows in principle the use of a Markov-chain Montecarlo method with a complexity that grows only linearly with the system size. We will not pursue this strategy here, which we leave for future studies.

In the following, we are interested in discussing the behavior of DNP protocols with trytil radicals, for which hyperfine couplings are weak and the stationary state of the electron spins is empirically found to be independent of the concentration of nuclear spins²⁸. This suggests that the occupation probability $p_{A,\mu}$ of having the nuclear spin system in the state $|A\rangle$ and the fermions in the many-body eigenstate $|\mu\rangle$ can be factorized, $p_{A,\mu} = p_A \times p_\mu$. Then, in the limit of vanishing hyperfine interaction, we can assume that the electron system remains always in the stationary state, namely we can replace $p_\mu \rightarrow p_\mu^{\text{stat}}$ in (12). This allows us to trace out the electron degrees of freedom, thus obtaining a rate equation only for the nuclear spins. We now consider the two opposite limits of uncoupled nuclear spins and strongly coupled, ergodic nuclear spins.

Non-interacting nuclear spins.— In the absence of nuclear dipolar interactions, each nucleus can be treated separately. We can focus on a single core nucleus, j_0 , coupled to only one electron site, by taking $A_j = A_0 \delta_{j,j_0}$ in (2a). Summing over all the possible electron states, we obtain the total rate for the transition of the j_0 -th

Electron parameters

T_{1e} (s)	T_{2e} (s)	ω_{MW} (2 π GHz)	ω_1 (2 π kHz)
1	10^{-6}	93.86	25

Nuclear parameters

T_{1n} (s)	T_{2n} (s)	ω_n (2 π MHz)	A_0 (2 π kHz)
10^4	10^{-5}	20	4.47

TABLE I. Microscopic parameters modeling the system in a magnetic field of $B = 3.3$ T ($\omega_e = 93.9$ 2 π GHz) in contact with a thermal bath at a temperature $\beta^{-1} = 1.2$ K and the microwave irradiation with amplitude ω_1 . The hyperfine coupling is chosen small enough so that the transitions involving nuclei are slower than the relaxation time T_{1e} of electron spins: $A_0^2/(\omega_n^2 T_{2n}) \lesssim T_{1e}^{-1}$. This justifies the approximation $p_\mu \simeq p_\mu^{\text{stat}}$ at all times. Stationary polarizations only depend on $A_0^2 T_{1n}$.

nucleus $|\downarrow\rangle \rightarrow |\uparrow\rangle$ as

$$W_{\downarrow \rightarrow \uparrow}^{j_0} \equiv \sum_{\mu,\nu} p_\mu^{\text{stat}} W_{(\downarrow,\mu \rightarrow \uparrow,\nu)}^{j_0} = \Omega_{j_0}(\omega_n) \quad (19)$$

where the function $\Omega_j(\omega)$ is obtained in appendix B 2 and reads

$$\Omega_j(\omega) = \frac{A_j^2 T_{2n}}{4} \sum_{\alpha,\beta} |\phi_{\alpha,j}|^2 |\phi_{\beta,j}|^2 \times \left[\frac{P_B(\epsilon_\alpha) P_B(\epsilon_\beta)}{1 + T_{2n}^2 \omega^2} + \frac{(1 + P_B(\epsilon_\alpha))(1 - P_B(\epsilon_\beta))}{1 + T_{2n}^2 (\omega + \epsilon_\beta - \epsilon_\alpha)^2} \right] + \frac{h(\omega)}{T_{1n}}. \quad (20)$$

Similarly, one can see that $W_{\downarrow \rightarrow \uparrow}^j = \Omega_j(-\omega_n)$. In this way, we obtain the stationary polarization for the nucleus j_0 as: $(\Omega_{j_0}(\omega_n) - \Omega_{j_0}(-\omega_n)) / (\Omega_{j_0}(\omega_n) + \Omega_{j_0}(-\omega_n))$. Then, the core polarization, obtained by averaging over only the N_e nuclear spins, which are coupled with the electrons, is given by

$$P_n^{\text{core}} = \frac{1}{N_e} \sum_{j=1}^{N_e} \frac{\Omega_j(\omega_n) - \Omega_j(-\omega_n)}{\Omega_j(\omega_n) + \Omega_j(-\omega_n)}. \quad (21)$$

In this situation, the leakage process for core nuclear spins is much slower than ISS and PL processes. However, the bulk polarization $P_n = P_n^{\text{core}} \times N_e/N_n$ is very small as it results from the average over all the nuclear spins, which include $N_n - N_e$ with a negligible polarization.

Using the parameters given in Table I, we show in the left panel of Fig. 2 the resulting value for P_n^{core} as a function of the hopping parameter t . at fixed disorder strength: $w = 108(2\pi\text{MHz})$. The value of P_n^{core} strongly depends on the correlations between single-particle wavefunctions, as both ϕ_α and ϕ_β must have a significant amplitude on at least one common site j . To illustrate this effect, in Fig. 2 – left, we compare P_n^{core} with the po-

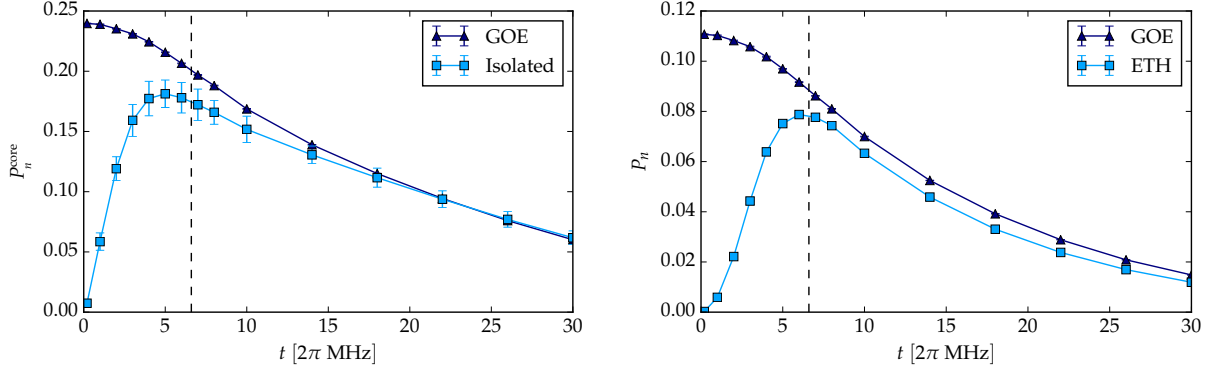


FIG. 2. (Color online) (left) Average core nuclear polarization (21) as a function of the hopping parameter t , for a non-interacting system of nuclei. (right) Average polarization in the ETH case (22) for a total of N_n nuclei, with N_e coupled a fermion site in the 3D Anderson Model. For both plots, the vertical line identifies the known Anderson transition. The linear size of the system is $L = 18$. Single-data are averaged over 60 realizations of the disorder and one standard deviation shown as error bars.

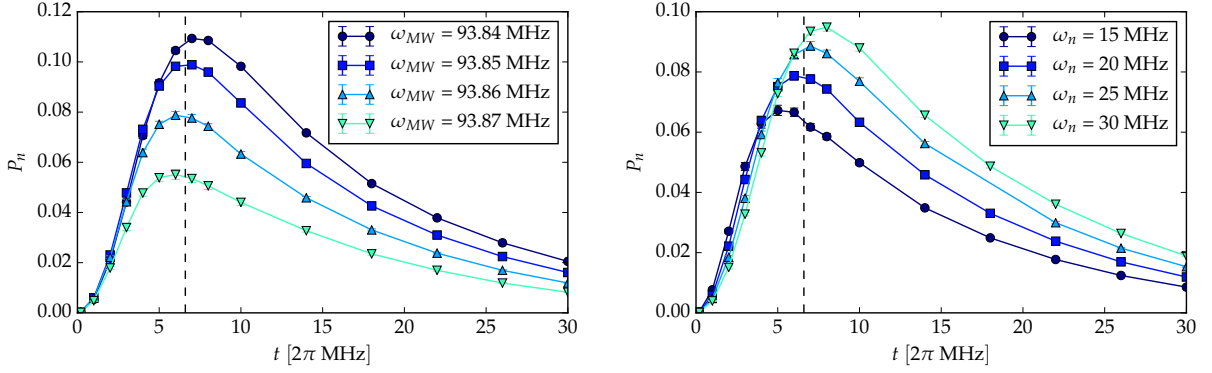


FIG. 3. (Color online) Average polarization in the ETH case (22) as a function of the hopping parameter. (left) different values of the microwave frequency ω_{MW} with fixed $\omega_n = 20$ MHz (left); (right) different values of ω_n with ω_{MW} given in Table I. For both plots, the vertical line identifies the known Anderson transition in the undriven system, assumin the fixed width of the box distribution of disorder, $w = 108(2\pi\text{MHz})$. The linear size of the system is $L = 18$. Each data point is obtained as an average over 60 realizations of the disorder and one standard deviation shown as error bars.

larization obtained assuming single-particle eigenvectors that are perfectly ergodic in the whole volume. In practice we keep the original values of ϵ_α 's but we replace the coefficients $\phi_{\alpha,i}$ coming from the diagonalization of M in (7), with those obtained by the diagonalization of a matrix in the Gaussian orthogonal ensemble (GOE). For large values of t , the polarization P_n^{GOE} obtained with this method agrees with P_n^{core} , showing a decaying behavior which we will discuss later. Approaching the transition, while P_n^{GOE} increases monotonously with decreasing t , P_n^{core} decays rapidly to zero. Indeed, the onset of localization at small t strongly suppresses the typical overlap between two single-particle wave functions with a resonant energy difference $\epsilon_\alpha - \epsilon_\beta \simeq \omega_n$. This will suppress the ISS rate, but not the loss rate, which although being off-resonance, collects contributions from all energy differences.

Ergodic nuclear spins.— In the presence of efficient nuclear dipolar interactions (which is usually the case in the experiments), we assume that statistical properties of nuclear many-body eigenstates are completely characterized by global conserved quantities, which in our case is only the total nuclear energy, \hat{H}_n . Therefore, it suffices to describe the evolution of the total energy of the nuclear system. For simplicity, we take the same hyperfine coupling $A_j = A_0$ in (2a) for all “core” nuclear spins that are coupled to the electrons, and set $A_j = 0$ for all other nuclei. Given that ω_n is much larger than the typical strength of dipolar coupling between nuclei, we assume that dipolar interactions are strong enough to render the nuclei ergodic, while contributing only a negligible broadening to the Zeeman gap ω_n . In this limit, the energy of a nuclear eigenstate $|A\rangle$ only depends on the number of up/down spins: $E_A = (N_+^{(A)} - N_-^{(A)})\omega_n/2$. Therefore,

the total rate of transitions that lower the nuclear energy by ω_n is $\sum_p \Omega_p(\omega_n)$, which includes also the contribution of nuclei not coupled to electron spins and that only undergo leakage processes. Thus, the total magnetization takes the form

$$P_n = \frac{\sum_p \Omega_p(\omega_n) - \Omega_p(-\omega_n)}{\sum_p \Omega_p(\omega_n) + \Omega_p(-\omega_n)}. \quad (22)$$

A derivation of this result including a non-trivial broadening due to the interactions is presented in appendix D using the Srednicki formula²⁹. Note that only for $p = 1, \dots, N_e$ the function $\Omega_p(\omega)$ given in (20) contains the contribution of the hyperfine interaction $A_p = A_0$; for the other nuclei, it reduces to the contribution coming from the leakage term (17), as $A_p = 0$.

In particular, in the ergodic regime of the nuclei, the microscopic details of the electron system determine the stationary nuclear polarization (22) only via the correlation function

$$\mathcal{K}(\epsilon, \epsilon') = \frac{1}{N_e} \sum_{\alpha, \beta, j} |\phi_{\alpha, j}|^2 |\phi_{\beta, j}|^2 \overline{\delta(\epsilon_\alpha - \epsilon) \delta(\epsilon_\beta - \epsilon')}, \quad (23)$$

which measures the overlap between eigenvectors at energies ϵ and ϵ' , and was discussed in detail in Ref. 30 in the context of Anderson localization. Using this expression in (22), we obtain

$$P_n = \frac{\frac{N_e}{4} \int d\epsilon d\epsilon' \mathcal{K}(\epsilon, \epsilon') \frac{P_B(\epsilon) - P_B(\epsilon')}{1 + T_{2n}^2 (\epsilon - \epsilon' + \omega_n)^2}}{\frac{N_e}{4} \int d\epsilon d\epsilon' \mathcal{K}(\epsilon, \epsilon') \frac{1 - P_B(\epsilon') P_B(\epsilon)}{1 + T_{2n}^2 (\epsilon - \epsilon' + \omega_n)^2} + \frac{2N_n}{A_0^2 T_{1n} T_{2n}}}, \quad (24)$$

where we neglected the contribution from the PL rate in (16), since it is subleading with respect to the leakage one in (17). Indeed, while the PL term only affects N_e core nuclei, the leakage affects all the N_n : in standard DNP conditions $N_n/N_e \simeq 10^3$ and we will use this value in the following.

In the right panel of Fig. 2, we show the behavior of the polarization in (22) as a function of the hopping parameter t . In the GOE, all the coefficients are of the same order, i.e. $|\phi_{\alpha i}|^2 \approx 1/N_e$ and

$$\mathcal{K}^{\text{GOE}}(\epsilon, \epsilon') = \rho(\epsilon) \rho(\epsilon'). \quad (25)$$

Using this approximation in (24), we obtain again a monotonous behavior for the polarization. Note that this GOE approximation differs from the one used in the calculation of “core” case, as all the nuclei contribute to the leakage rate, which is therefore $N_n/N_e = 10^3$ times larger. As before, we observe agreement between the two curves for $t \gg t_c$. However, at small values of t , leakage is responsible for a strong suppression and the nuclear polarization vanishes as $O(t^2)$. As a consequence, the maximal value of the polarization is reached for $t \simeq t_c$. In Fig. 3, this behavior is confirmed for a broad range of microwave frequencies ω_{MW} and nuclear Zeeman gaps

ω_n .

To gain further understanding, we show in Fig. (4) – left, the interplay between the different terms involved in the numerator and denominator of (24): in our regime of parameters, the denominator is always dominated by the leakage term (except at $t \simeq t_c$, where the two terms are of the same order, thus leading to a significative polarization). This suggests that the behavior of the polarization can be understood qualitatively by focusing on the numerator of (24). There, the contribution of the ISS process is strongly peaked at the resonant condition $\epsilon - \epsilon' \simeq \omega_n$, which leads to the approximate formula for the polarization

$$P_n \simeq P_n^{(0)} \int d\epsilon \mathcal{K}(\epsilon, \epsilon + \omega_n) (P_B(\epsilon) - P_B(\epsilon + \omega_n)), \quad (26)$$

with the constant $P_n^{(0)} = (\pi A_0^2 T_{1n} N_e) / (8 N_n)$. In the GOE approximation, we can use (25) and the dependence on t of the nuclear polarization can be explained by merely looking at the DOS. In Fig. 5, we show that the nuclear polarization depends on the asymmetry of the irradiation frequency ω_{MW} with respect to the DOS. Upon increasing t beyond the disorder level w , the density of electronic states is broadened. This has two effects (see Fig. 1): on the one hand, the asymmetry in the integrand becomes less and less pronounced, on the other hand the density of states itself becomes smaller, namely $\rho(\epsilon) \simeq O(t^{-1})$. This effect is insensitive to localization phenomena and is at play only as long as $t \gtrsim w$, that is, well into the ergodic phase.

In contrast, the eigenfunction correlator $\mathcal{K}(\epsilon, \epsilon')$ is affected by the onset of localization. To explain qualitatively its behavior, we remark that in the presence of a flat disorder distribution, as considered here, it depends essentially only on the energy difference as

$$\mathcal{K}(\epsilon, \epsilon + \omega) \simeq K(\omega), \quad K(\omega) = \int d\epsilon \mathcal{K}(\epsilon, \epsilon + \omega). \quad (27)$$

As one can check explicitly from (23), it must satisfy the sum rule

$$\int d\omega K(\omega) = 1. \quad (28)$$

To proceed further, it is convenient to define the *inverse participation ratio* (IPR) as

$$I_2 = \frac{1}{N_e} \sum_{\alpha, j} |\phi_{\alpha, j}|^4. \quad (29)$$

Once the localization transition is crossed, single-particle eigenstates have a support over a finite number of lattice sites whose number is measured by I_2^{-1} . Then, the overlap function $K(\omega)$ becomes singular at small ω , i.e. $K(\omega) = \delta(\omega) I_2 + \text{non-singular contributions}$. In Fig. 4 – right, we plot the behavior I_2 as a function of t . As at small t , the sum rule (28) is almost saturated by I_2 at

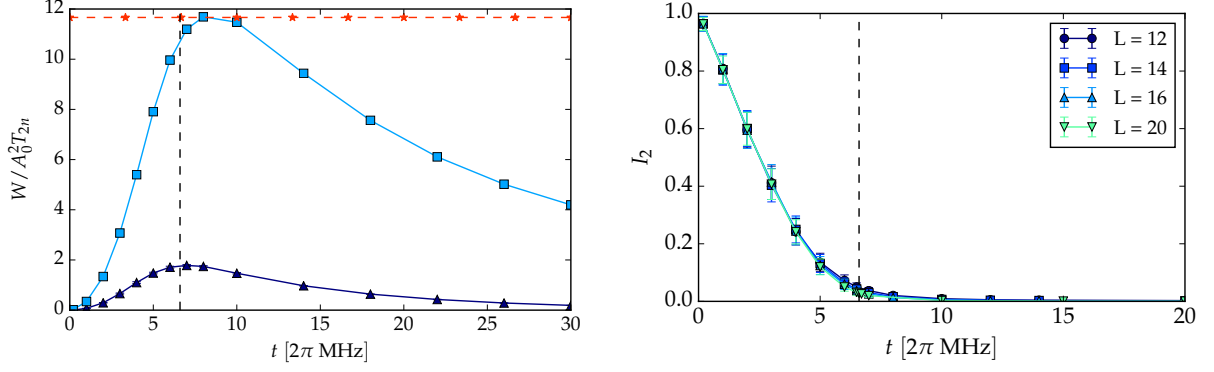


FIG. 4. (Color online) Left: Comparison between different terms in (24) as a function of t : the numerator (dark blue triangles), the first term in the denominator, corresponding to the ISS processes (light blue squares) and the second term, corresponding to constant leakage (red stars) $2N_n/(A_0^2 T_{1n} T_{2n})$. We observe that, except for $t \simeq t_c$, the most important contribution to the denominator comes from the leakage term. Right: Inverse partition ratio I_2 as a function of the hopping parameter for $L = 18$. I_2^{-1} measures the average number of sites occupied by a single-particle wave function. Therefore, I_2 becomes non-zero for $t < t_c$ signaling the AL transition.

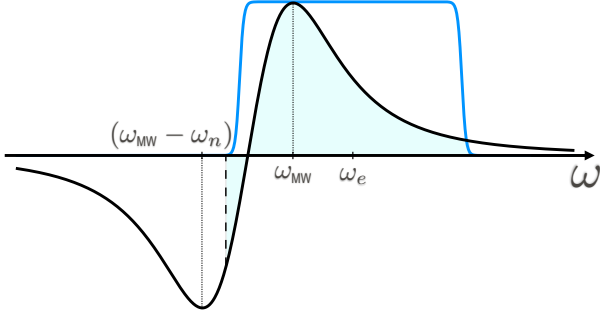


FIG. 5. (Color online) Sketch of the integrand in (26): $P_B(\epsilon) - P_B(\epsilon + \omega_n)$ (black) together with the DOS $\rho(\epsilon)$ (blue) (normalization is chosen for a clearer plot). The stationary polarization in the GOE approximation P_n^{GOE} is obtained as the integral over the domain where the DOS does not vanish. Upon increasing t , the integration window becomes larger and P_n^{GOE} decreases both because of the symmetry of the integrand and because of the total normalization of $\rho(\epsilon)$.

$\omega = 0$, $K(\omega)$ for $\omega \simeq \omega_n$ is suppressed. As a consequence, the number of ISS processes has a strong depletion once we cross the transition.

In the next section, we discuss the features of $K(\omega)$ that are reflected in the stationary nuclear polarization, especially close to the transition.

V. OVERLAP FUNCTION

It is useful to rescale the overlap function by the DOS, setting

$$C(\omega) = \frac{K(\omega)}{\int d\epsilon d\epsilon' \rho(\epsilon) \rho(\epsilon + \omega)}. \quad (30)$$

Then, using (26) and (27), we can estimate the nuclear polarization in (24) as the product

$$P_n \simeq C(\omega_n) \times P_n^{\text{GOE}} \quad (31)$$

where the GOE contribution captures the decay at large t , while $C(\omega_n)$ dominates the behavior at small t .

Far away from the critical point, $C(\omega)$ is constant, both for localized and extended eigenstates, as they are essentially uncorrelated. However, important deviations emerge in the critical regime around the localization transition $t \simeq t_c$. Remarkably, one can describe $C(\omega)$ in terms of a critical quantity D_2 computed exactly at $t = t_c$. At the critical point, single-particle wave functions are not localized and the IPR vanishes as $I_2 \simeq N_e^{-D_2}$. The exponent D_2 belongs to a whole family of critical exponents describing multifractality at the Anderson transition³². Then, the function $C(\omega)$ for $t \simeq t_c$ shows different regimes according to the value of ω ³¹:

$$C(\omega) \simeq \begin{cases} C_0(t) & \omega \ll \omega_0 \\ \left(\frac{\omega_0}{\omega}\right)^{1-D_2} & \omega_0 \ll \omega \ll E_0 \\ \left(\frac{E_0}{\omega}\right)^2 & \omega \gg E_0 \end{cases} \quad (32)$$

The power-law decay for intermediate values of ω corresponds to the critical region³³. E_0 indicates the upper cut-off for multifractality, where few-sites resonances become relevant for the overlap. A simple two-sites estimation leads to $E_0 \simeq 2t$. For $\omega \gg E_0$, one enters in the perturbative small t regime, where consistently one expects $C(\omega) \simeq t^2/\omega^2$. The other energy scale $\omega_0(t)$ indicates the beginning of the critical region³⁴. Its qualitative behavior is shown in Fig. 7. Numerical calculations of the function $C(\omega)$ are shown in Fig. 6 – left, as a function of the rescaled variable ω/t , confirming the scenario of (32): at large ω , data for different values of t perfectly overlap as

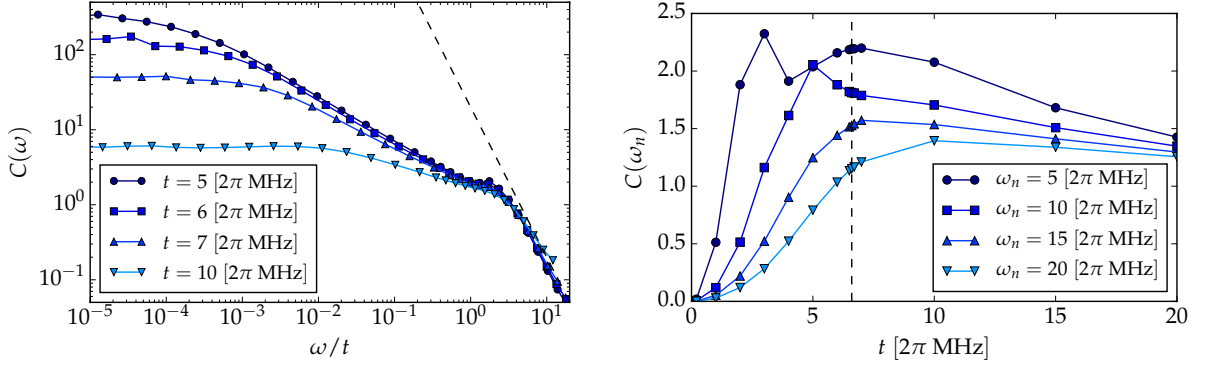


FIG. 6. (Color online) Left: Overlap function $C(\omega)$ as function of the rescaled variable ω/t for several values of t around the critical point t_c . The dashed line shows the power-law decay $\simeq (E_0/\omega)^2$ for comparison at large ω , where all functions have similar decay and overlap. For smaller ω , a power-law decay is observed in agreement with the critical scaling in (32). This region lasts longer for values of t closer t_c , where $\omega_0 \rightarrow 0$. Saturation to a constant value is expected at small $\omega \ll \delta_t$; small deviations from the flat saturation emerge in the localized region (see [31]). Right: Overlap function $C(\omega_n)$ as a function of t .

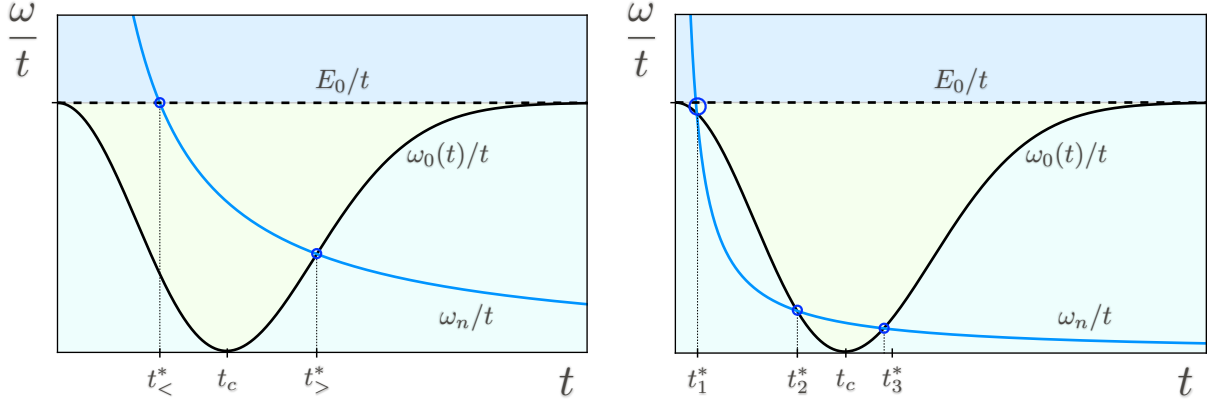


FIG. 7. (Color online) Sketch of the energy scales $\omega_0(t)/t$ (black), $E_0/t \simeq 2t$ (dashed black line) and ω_n/t , determining the regime of the function $C(\omega_n)$. On the left, large values of $\omega_n \gg 2t_c$, two intersections appear t^*_-, t^*_+ . On the right, small values $\omega_n \ll 2t_c$, three intersections t^*_1, t^*_2, t^*_3 explain the presence of two local maxima in $C(\omega_n)$ as a function of t (see Fig. 6 – right).

$E_0 \propto t$. For $t \gtrsim t_c$, the saturation to a t -dependent constant $C_0(t)$ at small ω is reminiscent of the GOE behavior $C^{\text{GOE}}(\omega) = 1$. For $t \lesssim t_c$, a similar saturation would be expected, but long-range resonances slightly enhance the overlap³¹; we will not consider this effect here. The function $C_0(t)$ decreases with t : because of the sum rule (28) satisfied by the overlap function, if t is decreased, a larger value $C_0(t)$ at the plateau is required to compensate the depletion occurring for $\omega \gg E_0 \sim 2t$. In the limit $t \rightarrow \infty$, $C_0(t) \rightarrow 1$, in agreement with the GOE prediction.

We can now use (31), together with (32) to understand the behavior of the polarization P_n for different values of ω_n (see Fig. 3 – right). We show in Fig. 6 – right, the numerical data for $C(\omega_n)$ as a function of t . Its shape can be inferred from (32). First of all, we observe that at small t , $\omega_n \gg 2t$, which explains the quadratic regime $C(\omega_n) \simeq t^2/\omega_n^2$. For larger t , one has to take into account that both scales $E_0 = 2t$ and $\omega_0 = \omega_0(t)$ depend on t : a

qualitative plot of these quantities is presented in Fig. 7. At the critical point, the critical region becomes larger, as $\omega_0 \rightarrow 0$; while when $t \gg t_c$, or $t \ll t_c$, the critical region shrinks to zero and $\omega_0 \rightarrow 2t \simeq E_0$. We must distinguish the two limits of small and large ω_n (as compared to the hopping t), respectively:

$\omega_n \gg 2t_c$. — In order to understand the behavior of $C(\omega_n)$ as a function t , we need to determine in which regime of the function in (32) one is. As discussed above, at small t 's, $\omega_n \gg E_0$. Then increasing, t , one enters in the critical region according to the solutions of $\omega_0(t^*)/t^* = \omega_n/t^*$. From Fig. 7 – left, we see that for large ω_n , there are two solutions $t^*_- < t^*_+$. Therefore, the critical region is reached when $t > t^*_-$: the function $C(\omega_n)$ changes its convexity and behaves as $C(\omega_n) \simeq (t/\omega_n)^{1-D_2}$. Then, for larger values, i.e. $t > t^*_+$, the critical regime is left and $C(\omega_n) = C_0(t)$, explaining the observed decay to 1 at large t in Fig. 6 – right.

$\omega_n \ll 2t_c$. — From Fig. 7 – right, we see that now we have three solutions $t_1^* < t_2^* < t_3^*$ for $\omega_0(t^*)/t^* = \omega_n/t^*$. Therefore, the function $C(\omega_n)$ decreases as $C_0(t)$ both for $t_1^* < t < t_2^*$ and $t > t_3^*$; in the intermediate region $t_2^* < t < t_3^*$, the critical region forces the growth $C(\omega_n) \simeq (t/\omega_n)^{1-D_2}$. This non-monotonous behavior, with two local maxima, is observed in Fig. (6) – right, for small values of ω_n .

Summarizing, the function $C(\omega_n)$ vanishes quadratically at small t 's, decreases to a 1 for large t , reaching a global maximum for $t \simeq t_c$. Going back to the polarization P_n , we observe a similar behavior, modified at large t 's where the decay of P_n^{GOE} in (31) leads to a vanishing polarization.

VI. CONCLUSION

In this work we presented a simplified approach to the dynamics of electron spins in the DNP protocol. It is based on an approximate mapping to the free-fermion 3D Anderson model, which allowed us to obtain exact results for the driven steady states in large systems. As the free fermion model is integrable, it fails to accurately describe the spin-temperature regime of an ergodic spin system. However, it exhibits a well-studied Anderson transition, which permits us to study the influence of localization phenomena on the stationary nuclear polarization. Remarkably, in a broad range of physical parameters relevant for DNP experiments, the optimal polarization is reached close to the localization transition. Thus, we confirm the results obtained in [18] for much smaller, but interacting systems. Moreover, we find an explicit relation

between the nuclear polarization and the eigenfunction correlations of the fermions, which provides non-trivial insight into the associated crossover of steady states, as the spin system undergoes a localization transition. Our result suggests how DNP can in fact be used as a diagnostic tool to investigate localization physics both in the presence and in the absence of interactions.

Our work opens several interesting directions: while here the dynamics of electron spins was frozen to their stationary state in absence of nuclei at any time, it is interesting to explore different regimes, where the effect of nuclei on the electron spins cannot be neglected. In particular, it is conceivable that for sufficiently strong hyperfine interactions, an ergodic system of nuclei leads to the delocalization of the electron spins. As we pointed out, this situation can be approached within our framework by means of a Montecarlo simulation, which will be analyzed in a forthcoming publication.

Moreover, in this work, nuclear spins were supposed to be a perfectly ergodic system, thus assuming that nuclear spin diffusion occurs on a time scale that is much faster than all the other nuclear processes. Extending our approach to include a finite nuclear spin-diffusion time is a challenging direction, which requires a more sophisticated approach and will be addressed in future research.

ACKNOWLEDGMENTS

This work is supported by the EPSRC Quantum Matter in and out of Equilibrium grant Ref. EP/N01930X/1 (A.D.L.), Investissements d'Avenir LabEx PALM (ANR-10-LABX-0039-PALM), and ANR-16-CE30-0023- 01 (THERMOLOC).

-
- ¹ D. Basko, I. Aleiner, and B. Altshuler, *Ann. Phys.* **321**, 1126 (2006).
 - ² M. Schreiber, S. S. Hodgman, P. Bordia, H. P. Lüschen, M. H. Fischer, R. Vosk, E. Altman, U. Schneider, and I. Bloch, *Science* **349**, 842 (2015).
 - ³ P. Bordia, H. P. Lüschen, S. S. Hodgman, M. Schreiber, I. Bloch, and U. Schneider, *Physical review letters* **116**, 140401 (2016).
 - ⁴ J. Smith, A. Lee, P. Richerme, B. Neyenhuis, P. W. Hess, P. Hauke, M. Heyl, D. A. Huse, and C. Monroe, *Nature Physics* **12**, 907 (2016).
 - ⁵ A. Pal and D. A. Huse, *Phys. Rev. B* **82**, 174411 (2010).
 - ⁶ R. Vosk and E. Altman, *Phys. Rev. Lett.* **110**, 067204 (2013).
 - ⁷ M. Serbyn, Z. Papić, and D. A. Abanin, *Physical review letters* **111**, 127201 (2013).
 - ⁸ A. De Luca and A. Scardicchio, *Europhys. Lett.* **101**, 37003 (2013).
 - ⁹ D. J. Luitz, N. Laflorencie, and F. Alet, *Physical Review B* **91**, 081103 (2015).
 - ¹⁰ V. Ros, M. Müller, and A. Scardicchio, *Nuclear Physics B* **891**, 420 (2015).
 - ¹¹ M. Pino, L. B. Ioffe, and B. L. Altshuler, *Proceedings of the National Academy of Sciences* **113**, 536 (2016).
 - ¹² J. Z. Imbrie, *Journal of Statistical Physics* **163**, 998 (2016).
 - ¹³ R. Nandkishore, S. Gopalakrishnan, and D. A. Huse, *Phys. Rev. B* **90**, 064203 (2014).
 - ¹⁴ M. H. Fischer, M. Maksymenko, and E. Altman, *Physical review letters* **116**, 160401 (2016).
 - ¹⁵ E. Levi, M. Heyl, I. Lesanovsky, and J. P. Garrahan, *Physical Review Letters* **116**, 237203 (2016).
 - ¹⁶ M. Marcuzzi, J. Minář, D. Barredo, S. de Léséleuc, H. Labuhn, T. Lahaye, A. Browaeys, E. Levi, and I. Lesanovsky, *Physical Review Letters* **118**, 063606 (2017).
 - ¹⁷ A. De Luca and A. Rosso, *Phys. Rev. Lett.* **115**, 080401 (2015).
 - ¹⁸ A. De Luca, I. Rodríguez-Arias, M. Müller, and A. Rosso, *Physical Review B* **94**, 014203 (2016).
 - ¹⁹ F. Caracciolo, M. Filibian, P. Carretta, A. Rosso, and A. De Luca, *Physical Chemistry Chemical Physics* **18**, 25655 (2016).
 - ²⁰ M. Borghini, *Phys. Rev. Lett.* **20**, 419 (1968).
 - ²¹ A. Abragam and M. Goldman, *Nuclear Magnetism: Order and Disorder* (Oxford University Press, 1982).

- ²² F. Petruccione and H.-P. Breuer, *The theory of open quantum systems* (Oxford Univ. Press, 2002).
- ²³ Y. Hovav, A. Feintuch, and S. Vega, *J. Magn. Reson.* **214**, 29 (2012).
- ²⁴ Y. Hovav, A. Feintuch, and S. Vega, *Phys. Chem. Chem. Phys.* **15**, 188 (2013).
- ²⁵ A. Karabanov, A. van der Drift, L. J. Edwards, I. Kuprov, and W. Köckenberger, *Phys. Chem. Chem. Phys.* **14**, 2658 (2012).
- ²⁶ A. Karabanov, D. Wiśniewski, I. Lesanovsky, and W. Köckenberger, *Physical Review Letters* **115**, 020404 (2015), arXiv:1503.04357 [quant-ph].
- ²⁷ K. Slevin and T. Ohtsuki, *New Journal of Physics* **16**, 015012 (2014).
- ²⁸ S. Colombo Serra, M. Filibian, P. Carretta, A. Rosso, and F. Tedoldi, *Phys. Chem. Chem. Phys.* **16**, 753 (2014).
- ²⁹ M. Srednicki, *Journal of Physics A: Mathematical and General* **32**, 1163 (1999).
- ³⁰ E. Cuevas and V. Kravtsov, *Physical Review B* **76**, 235119 (2007).
- ³¹ E. Cuevas and V. Kravtsov, *Physical Review B* **76**, 235119 (2007).
- ³² F. Evers and A. D. Mirlin, *Reviews of Modern Physics* **80**, 1355 (2008).
- ³³ J. Chalker, *Physica A: Statistical Mechanics and its Applications* **167**, 253 (1990).
- ³⁴ For $t < t_c$ it corresponds to the mean-level spacing in a localization volume, which can be estimated combining the IPR with the DOS as $\omega_0 \simeq I_2/\rho(\omega_e)$.

Appendix A: Diagonalization of the 3D-Anderson Model Hamiltonian

The starting point for the free fermions model for the electron spins is the Hamiltonian in equation (2a), including the term that accounts for the dipolar interactions :

$$\hat{H}_e^{(dip)} = \sum_{i < j} \sum_{\ell=x,y,z} D_{ij} \hat{S}_i^\ell \hat{S}_j^\ell, \quad (\text{A1})$$

which is analogous to the dipolar coupling between nuclear pairs of spins. The exact form of those dipolar couplings between two spins \hat{S}_i, \hat{S}_j with respective gyromagnetic ratios γ_i, γ_j - being γ_e for an electron spin and γ_n for a nuclear one - reads :

$$D_{ij} = \frac{\mu_0 \gamma_1 \gamma_2}{16\pi |\mathbf{r}_{ij}|^3} (1 - 3 \cos^2 \theta_{ij}), \quad (\text{A2})$$

with \mathbf{r}_{ij} the vector connecting the two spins and θ_{ij} the angle that this vector forms with the external magnetic field. Note that the expression in Eq (A2) varies strongly from pair to pair.

At this point one performs the *spin-to-fermion* transformation given in Eq. (5), which results in a quadratic fermionic Hamiltonian

$$\hat{H}_{\text{Ferm}} = \sum_{i,j} c_i^\dagger M_{ij} c_j, \text{ with } M_{ij} = \omega_j \delta_{ij} + D_{ij}, \quad (\text{A3})$$

after a renormalization of the zero of energy and the Zeeman frequencies ω_j . Additionally, we have neglected the interaction term coming from the dipolar coupling, retaining only the hopping term. We consider only a constant hopping term between nearest neighbors assuming $D_{ij} = -t \delta_{i \pm 1, j}$ in Eq. (A3), which finally leads to the 3D-Anderson Model introduced in (6). Numerical diagonalization of the matrix M_{ij} is performed and we set $\phi_{\alpha i}$ as the single-particle wave-function, i.e. the eigenvector of the matrix M_{ij} with eigenvalue ϵ_α . This is equivalent to set $a_\alpha = \sum_i \phi_{\alpha i}^* c_i$, or equivalently $c_i = \sum_\alpha \phi_{\alpha i} a_\alpha$. The Hamiltonian (A3) thus becomes

$$\hat{H}_{\text{ferm}} = \sum_{i,j} \sum_{\alpha\beta} \epsilon_\alpha c_i^\dagger \phi_{\alpha i} \delta_{\alpha\beta} \phi_{\beta j}^* c_j = \sum_{\alpha} \epsilon_\alpha a_\alpha^\dagger a_\alpha. \quad (\text{A4})$$

The coefficients are normalized as $\sum_i \phi_{\alpha i}^* \phi_{\beta i} = \delta_{\alpha\beta}$.

Appendix B: Microscopic derivation of the transition rates

1. Lattice and microwave-induced rates for the free fermions

The explicit expressions for the transition rates induced by the reservoir and the microwaves can be obtained making some assumptions: We consider on the one hand that the lattice modes couple to local electronic spins only. This

means that it can induce spin flips always respecting detailed balance at the temperature of the bath β^{-1} . The rates can be derived as in [17] and then we can perform the *spin-to-fermion* substitution in (5)

$$W_{\mu \rightarrow \nu}^{\text{bath}} = \sum_{\substack{j=1 \\ \ell=x,y}}^{N_e} 2 \frac{h(\Delta E_{\mu\nu})}{T_{1e}} |\langle \mu | \hat{S}_j^\ell | \nu \rangle|^2 \rightarrow \sum_{j=1}^{N_e} \frac{h(\Delta E_{\mu\nu})}{T_{1e}} |\langle \mu | (c_j^\dagger + c_j) | \nu \rangle|^2 = \sum_{\alpha} \frac{h(\Delta E_{\mu\nu})}{T_{1e}} |\langle \mu | (a_\alpha^\dagger + a_\alpha) | \nu \rangle|^2. \quad (\text{B1})$$

The function $h(\epsilon) = e^{\beta\epsilon}/(1+e^{\beta\epsilon})$ assures the Gibbs equilibrium at temperature β^{-1} when the system is not irradiated; T_{1e} is the typical time that the bath takes to induce a spin flip in the system and $\Delta E_{\mu\nu} = E_\mu - E_\nu$.

On the other hand, the system is being irradiated with the microwave field $\hat{H}_{\text{MW}} = \omega_1 \sum_j \hat{S}_j^x \cos(\omega_{\text{MW}} t)$. This Hamiltonian is time-dependent, but one can perform the *rotating-wave approximation* that neglects the fast-oscillating terms. In [17] the following rate for the microwave-induced transitions was obtained as :

$$W_{\mu \rightarrow \nu}^{\text{MW}} = \frac{4\omega_1^2 T_{2e}}{1 + T_{2e}^2(|\Delta E_{\mu\nu}| - \omega_{\text{MW}})^2} |\langle \mu | \sum_{j=1}^{N_e} \hat{S}_j^x | \nu \rangle|^2. \quad (\text{B2})$$

Then one performs again the *spin-to-fermion* substitution in equation (5).

$$W_{\mu \rightarrow \nu}^{\text{MW}} = \frac{\omega_1^2 T_{2e}}{1 + T_{2e}^2(|\Delta E_{\mu\nu}| - \omega_{\text{MW}})^2} |\langle \mu | \sum_{j=1}^{N_e} (c_j^\dagger + c_j) | \nu \rangle|^2 = \sum_{\alpha} \frac{T_{2e} \omega_1^2 |A_\alpha|^2}{1 + T_{2e}^2(|\Delta E_{\mu\nu}| - \omega_{\text{MW}})^2} |\langle \mu | a_\alpha^\dagger + a_\alpha | \nu \rangle|^2, \quad (\text{B3})$$

with $A_\alpha = \sum_i \phi_{\alpha,i}$. Note that the rate of bath induced transitions (B1) is given by the sum of independent single spin flips. Unlike microwaves which induce transition on the total spin $\sum_j \hat{S}_j^z$. As a consequence, the microwave intensity ω_1 is renormalized to $\omega_1 |A_\alpha|$. In absence of interactions it is easy to check that $|A_\alpha| = 1$. In the regime where (5) is applicable, the hopping term $D_{ij} \ll \omega_j$, so that $A_\alpha \simeq 1$; for larger values of the hopping term, they exhibit unphysical fluctuations (although in average over α it remains true that $A_\alpha = 1$), which is a manifestation of the breaking in the naïve replacement stated in (5). Consistently with our assumptions of weak dipolar coupling, we set from now on $|A_\alpha| = 1$.

2. Hyperfine-induced rates: a single nuclear spin

We are now interested in computing the transition rates induced by the presence of a single nuclear spin (labeled by the index p) weakly coupled to the electron spin at site j . We thus take the Hamiltonian in (2b), which induces on the one hand a nuclear spin flip $i_z \rightarrow \bar{i}_z$ and, on the other hand - due to the fact that expectation values of the local \hat{S}_j^z operators are no longer conserved quantities - a change on the fermionic eigenstate.

$$\begin{aligned} W_{i_z \mu \rightarrow \bar{i}_z \nu} &= \frac{T_{2n}}{1 + T_{2n}^2 (2i_z \omega_n + E_\mu - E_\nu)^2} |\langle \mu, i_z | \hat{H}_{e-n} | \nu, \bar{i}_z \rangle|^2 \\ &= \frac{T_{2n} A_{jp}^2}{1 + T_{2n}^2 (2i_z \omega_n + E_\mu - E_\nu)^2} |\langle \mu, i_z | \hat{\mathcal{I}}_x (c_j^\dagger c_j - 1/2) | \nu, \bar{i}_z \rangle|^2 \\ &= \frac{T_{2n} A_{jp}^2}{1 + T_{2n}^2 (2i_z \omega_n + E_\mu - E_\nu)^2} |\langle \mu | (c_j^\dagger c_j - 1/2) | \nu \rangle|^2 |\langle i_z | \hat{\mathcal{I}}_x | \bar{i}_z \rangle|^2 \\ &= \frac{T_{2n} A_{jp}^2 / 4}{1 + T_{2n}^2 (2i_z \omega_n + E_\mu - E_\nu)^2} |\langle \mu | (c_j^\dagger c_j - 1/2) | \nu \rangle|^2, \end{aligned} \quad (\text{B4})$$

The only matrix element that requires a little care computing is:

$$\begin{aligned} \langle \mu | \left(c_j^\dagger c_j - \frac{1}{2} \right) | \nu \rangle &= \sum_{\alpha\beta} \phi_{\alpha,j}^* \phi_{\beta,j} \langle \mu | \left(a_\alpha^\dagger a_\beta - \frac{\delta_{\alpha,\beta}}{2} \right) | \nu \rangle = \\ &= \sum_{\alpha} \delta_{\mu,\nu} |\phi_{\alpha,j}|^2 \left(n_\alpha^\nu - \frac{1}{2} \right) + \sum_{\alpha,\beta \neq \alpha} \phi_{\alpha,j}^* \phi_{\beta,j} (1 - n_\alpha^\nu) n_\beta^\nu n_\alpha^\mu (1 - n_\beta^\mu) \prod_{\gamma \neq \alpha,\beta} \delta_{n_\gamma^\nu n_\gamma^\mu}. \end{aligned} \quad (\text{B5})$$

As we see, the total number of fermions is conserved. Two transitions are activated :

- A *leakage* transition which flips only the nuclear spin and leaves the fermionic eigenstate unchanged. The rate of this process is:

$$W_{i_z \mu \rightarrow \bar{i}_z \mu}^{\text{leak}} = \frac{T_{2n} A_{jp}^2}{1 + T_{2n}^2 \omega_n^2} \sum_{\alpha, \beta} |\phi_{\alpha, j}|^2 |\phi_{\beta, j}|^2 \left(n_\alpha^\mu - \frac{1}{2} \right) \left(n_\beta^\mu - \frac{1}{2} \right) \equiv \frac{T_{2n} A_{jp}^2}{1 + T_{2n}^2 \omega_n^2} \left[\sum_{\alpha} |\phi_{\alpha, j}|^2 \left(n_\alpha^\mu - \frac{1}{2} \right) \right]^2, \quad (\text{B6})$$

- A *ISS* transition which flips the nuclear spin exchanges the occupation number of two single particle fermionic modes (one being empty and the other full and vice-versa). The corresponding rate writes :

$$W_{i_z \mu \rightarrow \bar{i}_z \nu \neq \mu}^{\text{ISS}} = \frac{T_{2n} A_{jp}^2}{1 + T_{2n}^2 (2i_z \omega_n + E_\mu - E_\nu)^2} \sum_{\alpha, \beta \neq \alpha} |\phi_{\alpha, j}|^2 |\phi_{\beta, j}|^2 (1 - n_\alpha^\nu) n_\beta^\nu n_\alpha^\mu (1 - n_\beta^\mu) \prod_{\gamma \neq \alpha, \beta} \delta_{n_\gamma^\nu n_\gamma^\mu}. \quad (\text{B7})$$

Appendix C: Derivation of the nuclear polarization in absence of nuclear dipolar interactions

For the sake of simplicity we restrict to the contact term of the hyperfine interactions $A_{jp} = A_j \delta_{jp}$. Thus, in absence of nuclear dipolar interactions, a nucleus hyperpolarizes only in proximity of an electron spin j . Thus we can write the following master equation:

$$\dot{p}_{i_z, \mu}^j = \sum_{\nu} p_{i_z, \nu}^j W_{i_z \nu \rightarrow i_z \mu}^j - p_{i_z, \mu}^j W_{i_z \mu \rightarrow \bar{i}_z \nu}^j + \sum_{\nu} p_{i_z, \nu}^j W_{i_z \nu \rightarrow i_z \mu}^j - p_{i_z, \mu}^j W_{i_z \mu \rightarrow i_z \nu}^j \quad (\text{C1})$$

where $p_{i_z, \mu}^j$ is the probability of having the nucleus in proximity to the electron j in the state i_z and the fermions in the many-body eigenstate $|\mu\rangle$. By summing over the possible electron states $|\mu\rangle$, we obtain the probability for the nucleus of being in the state i_z : $p_{i_z}^j = \sum_{\mu} p_{i_z, \mu}^j$. The second sum in Eq. (C1) contains only transitions which do not change the state of the nucleus and are eliminated by the sum over $|\mu\rangle$. Then we have

$$\dot{p}_{i_z}^j = \sum_{\mu \nu} p_{i_z, \nu}^j W_{i_z \nu \rightarrow i_z \mu}^j - p_{i_z, \mu}^j W_{i_z \mu \rightarrow \bar{i}_z \nu}^j = \sum_{\mu \nu} p_{i_z, \mu}^j W_{i_z \mu \rightarrow i_z \nu}^j - p_{i_z, \mu}^j W_{i_z \mu \rightarrow \bar{i}_z \nu}^j \quad (\text{C2})$$

In the stationary limit, we set $\dot{p}_{i_z}^j = 0$ and make the additional assumption -well justified for trityl electron radicals- that the dynamics of the nucleus does not affect the electron stationary state: this suggests the factorization $p_{i_z, \mu}^j = p_{i_z}^j \times p_\mu$, where p_μ is the probability of having the fermions in the many-body eigenstate $|\mu\rangle$. Let us define the transition rate $W_{i_z \rightarrow \bar{i}_z}^j = \sum_{\mu, \nu} p_\mu W_{i_z \mu \rightarrow \bar{i}_z \nu}^j = \Omega_j (2i_z \omega_n)$, with

$$\Omega_j(\omega) = \sum_{\mu, \nu} \frac{A_j^2 T_{2n} p_\mu}{1 + T_{2n}^2 (\omega + E_\mu - E_\nu)^2} \sum_{\alpha, \beta} |\phi_{\alpha, j}|^2 |\phi_{\beta, j}|^2 \left[\delta_{\mu \nu} \left(n_\alpha^\nu - \frac{1}{2} \right) \left(n_\beta^\nu - \frac{1}{2} \right) + (1 - n_\alpha^\nu) n_\beta^\nu n_\alpha^\mu (1 - n_\beta^\mu) \prod_{\gamma \neq \alpha, \beta} \delta_{n_\gamma^\nu n_\gamma^\mu} \right] \quad (\text{C3})$$

It is convenient to replace the single-particle occupation numbers of a given many-body eigenstate with the polarization of the original spin model, namely $P_\alpha^\mu = 2n_\alpha^\mu - 1$ (which is either ± 1) :

$$\Omega_j(\omega) = \frac{A_j^2 T_{2n}}{4} \sum_{\alpha, \beta} |\phi_{\alpha, j}|^2 |\phi_{\beta, j}|^2 \sum_{\mu} p_\mu \left[\frac{(P_\alpha^\mu)^2 \delta_{\alpha, \beta} + P_\alpha^\mu P_\beta^\mu (1 - \delta_{\alpha, \beta})}{1 + T_{2n}^2 \omega^2} + \frac{(1 + P_\alpha^\mu)(1 - P_\beta^\mu)}{1 + T_{2n}^2 (\omega + \epsilon_\alpha - \epsilon_\beta)^2} \right] \quad (\text{C4})$$

The first term represents the *leakage* whereas the second one represents the *ISS* transition and involves the hopping of a fermion from the single-particle mode α to the single-particle mode β , thus the difference of energy reduces to $\Delta E_{\mu \nu} = \epsilon_\alpha - \epsilon_\beta$. In the stationary state $p_\mu \rightarrow p_\mu^{\text{st}}$ and $\sum_{\mu} p_\mu^{\text{st}} P_\alpha^\mu = P_B(\epsilon_\alpha)$, where $P_B(\epsilon_\alpha)$ is the Bloch polarization

defined in equation (11). We finally obtain :

$$\Omega_j(\omega) = \frac{A_j^2 T_{2n}}{4} \sum_{\alpha, \beta} |\phi_{\alpha, j}|^2 |\phi_{\beta, j}|^2 \times \left[\frac{\delta_{\alpha, \beta} + P_B(\epsilon_\alpha) P_B(\epsilon_\beta) (1 - \delta_{\alpha, \beta})}{1 + T_{2n}^2 \omega^2} + \frac{(1 + P_B(\epsilon_\alpha))(1 - P_B(\epsilon_\beta))(1 - \delta_{\alpha, \beta})}{1 + T_{2n}^2 (\omega + \epsilon_\beta - \epsilon_\alpha)^2} \right], \quad (\text{C5})$$

which has been simplified as equation (20) removing the vanishing contribution of the $\delta_{\alpha\beta}$ terms. At the end, we obtain that the nuclear polarization writes:

$$P_n^j = \frac{\Omega_j(\omega_n) - \Omega_j(-\omega_n)}{\Omega_j(\omega_n) + \Omega_j(-\omega_n)} = \frac{\sum_{\alpha\beta} |\phi_{\alpha, j}|^2 |\phi_{\beta, j}|^2 \times \frac{P_\beta - P_\alpha}{1 + T_{2n}^2 (\epsilon_\beta - \epsilon_\alpha + \omega_n)^2}}{\sum_{\alpha\beta} |\phi_{\alpha, j}|^2 |\phi_{\beta, j}|^2 \left(\frac{P_\alpha P_\beta}{1 + T_{2n}^2 \omega_n^2} + \frac{1 - P_\alpha P_\beta}{1 + T_{2n}^2 (\epsilon_\beta - \epsilon_\alpha + \omega_n)^2} \right)} \quad (\text{C6})$$

Appendix D: Derivation of the nuclear polarization for nuclei in the ETH phase

At this point we want to compute the nuclear polarization of a fast dipolar-interacting system of nuclear spins. In this case, the only conserved quantities are the total energy and the total magnetization of the nuclear spins. This corresponds to the Eigenstate Thermalization Hypothesis regime (ETH). According to this hypothesis, we can assume that the matrix element of the local operator \hat{I}_p^x between two nuclear eigenstates labeled by $|A\rangle$ and $|B\rangle$ takes the form

$$\langle A | \hat{I}_p^x | B \rangle = e^{-S(E_{AB})/2} f(E_{AB}, \Delta E_{AB}) R_{AB} \quad (\text{D1})$$

where $E_{AB} = (E_A + E_B)/2$, $S(E)$ is the entropy and R_{AB} contains all the fluctuations, being Gaussian random variables with zero average and unit variance. In the following, we set $R_{AB}^2 = 1$ for simplicity. As before, we want now to compute the probability for the nuclear system to be at a given energy E . We define

$$p(E) = e^{-S(E)} \sum_{A|E_A=E} p_A = e^{-S(E)} \sum_{A|E_A=E} \sum_{\mu} p_{A, \mu} \quad (\text{D2})$$

and again we make the assumption $p_{A, \mu} = p_A p_\mu$. We can perform a semi-classical integration that leads us to:

$$\begin{aligned} \dot{p}(E) &= e^{-S(E)} \int dE' \sum_{\substack{A|E_A=E \\ B|E_B=E'}} \sum_{\mu, \nu} (p_B p_\mu W_{(\mu, B) \rightarrow (\nu, A)} - p_A p_\mu W_{(\mu, A) \rightarrow (\nu, B)}) = \\ &= e^{-S(E)} \sum_j \int dE' \sum_{\substack{A|E_A=E \\ B|E_B=E'}} |\langle A | I_x^q | B \rangle|^2 (p_B \Omega_j(-\Delta E_{AB}) - p_A \Omega_j(\Delta E_{AB})) = \\ &= e^{-S(E)} \sum_j \int d\omega \sum_{\substack{A|E_A=E \\ B|E_B=E+\omega}} e^{-S(E+\omega/2)} f(E + \omega/2, \omega)^2 (p_B \Omega_j(-\omega) - p_A \Omega_j(\omega)) = \\ &= \sum_j \int d\omega e^{S(E+\omega) - S(E+\omega/2)} f(E + \omega/2, \omega)^2 (p(E + \omega) \Omega_j(-\omega) - p(E) \Omega_j(\omega)) \end{aligned} \quad (\text{D3})$$

In order to fix the function $f(E, \omega)$, we compute the two-point correlation for an arbitrary observable $\hat{O} = \hat{O}_D + \delta\hat{O}$ where \hat{O}_D is the diagonal component. We have

$$\begin{aligned} \frac{1}{Z} \text{Tr}[e^{-\beta H} \delta\hat{O}(t) \delta\hat{O}(0)] &= \sum_{\mu, \nu} e^{-\beta E_\mu} e^{i(E_\mu - E_\nu)t} |\langle \mu | \delta\hat{O} | \nu \rangle|^2 = \\ &= \sum_{\mu, \nu} e^{-\beta E_\mu} e^{i(E_\mu - E_\nu)t} e^{-S(E)} |f(E, \omega)|^2 R_{\mu\nu}^2 \simeq \int dE e^{-\beta E + \beta \omega/2 + S(E)} \int d\omega |f(E, \omega)|^2 e^{i\omega t} \simeq \int d\omega |f(E_\beta, \omega)|^2 e^{(\beta/2 + it)\omega} \end{aligned} \quad (\text{D4})$$

Applying this formula to the specific case $\delta\hat{O} = \hat{I}_x^q$ we have

$$\int d\omega |f(E, \omega)|^2 e^{(\beta/2 + it)\omega} = \frac{1}{Z} \text{Tr}[e^{-\beta E H_N} I_x^q(t) I_x^q] \quad (\text{D5})$$

where H_N is the Hamiltonian of the nuclear system (including the dipolar interactions), and E is the average energy associated with the temperature β_E^{-1} : $Z^{-1} \text{Tr}[e^{-\beta_E \hat{H}_N} \hat{H}_N] = E$. In this way the function $f(E, \omega)$ is simply connected to the Fourier-transform of the two-point correlation function of the I_x^q operator. Note that such a correlation function can be accessed experimentally in the linear response regime.

As E is a macroscopic energy, we can approximate $S(E + \omega/2) \simeq S(E) + S'(E)\omega/2$, with $S'(E) = \beta_E$ and we arrive at

$$\dot{p}(E) = \sum_j \int d\omega e^{\beta_E \omega/2} |f(E, \omega)|^2 (p(E + \omega)\Omega_j(-\omega) - p(E)\Omega_j(\omega)) \quad (\text{D6})$$

This equation is valid for an arbitrary nuclear system under the hypothesis of ETH, i.e. Eq. (D1) and only requires the knowledge of $f(E, \omega)$. If we now assume that the dipolar coupling between nuclei is sufficient to establish an ETH, but negligible with respect to their Zeeman gap ω_n , we can estimate $f(E, \omega)$ from the correlation function computed in absence of interactions

$$\frac{1}{Z} \text{Tr}[e^{-\beta_E H_N} I_x^q(t) I_x^q] = \frac{\cosh((\beta_E + it)\omega_n/2)}{\cosh(\beta_E \omega_n/2)} \Rightarrow |f(E, \omega)|^2 = \frac{\delta(\omega - \omega_n) + \delta(\omega + \omega_n)}{2 \cosh(\beta_E \omega_n/2)} \quad (\text{D7})$$

which is peaked around the frequencies $\pm\omega_n$. Here, we have associated to the microcanonical energy E the corresponding canonical β_E using

$$E = \int dE' p(E') E' = \frac{N_n \omega_n \tanh(\beta_E \omega_n/2)}{2} \quad (\text{D8})$$

Injecting (D7) in (D6), we can now look for the stationary solution of (D6) (i.e. $\dot{p}(E) = 0$), which requires

$$\frac{p(E + \omega_n)}{p(E)} = \frac{\sum_j \Omega_j(\omega_n)}{\sum_j \Omega_j(-\omega_n)} \Rightarrow P_n = \frac{\sum_j \Omega_j(\omega_n) - \Omega_j(-\omega_n)}{\sum_j \Omega_j(\omega_n) + \Omega_j(-\omega_n)} \quad (\text{D9})$$

which is the formula used in Eq. (22) in the main text.

A simpler way to derive this result in this approximation would be to assume that the eigenstates $|A\rangle$ of the nuclear Hamiltonian with a given number N_+ of spins up take the form

$$|A\rangle = \frac{1}{(\mathcal{N}_+)^{1/2}} \sum_{s=1}^{\mathcal{N}_+} c_s^A |s\rangle, \quad \mathcal{N}_+ = \binom{N_n}{N_+} \quad (\text{D10})$$

where the sum over s runs over all the \mathcal{N}_+ factorized configurations with N_+ spins up and c_s^A are random coefficients with zero average and variance 1 and for simplicity we set $(c_s^A)^2 = 1$. Then, one can explicitly compute the matrix element in (D1) which is non-vanishing only when $N_A^+ = N_B^+ \pm 1$. This leads to the master equation in the large N_n limit

$$\dot{p}(E) = \frac{N_+}{N_n} \sum_j [p(E + \omega_n)\Omega_j(\omega_n) - p(E)\Omega_j(-\omega_n)] + \left(1 - \frac{N_+}{N_n}\right) \sum_j [p(E - \omega_n)\Omega_j(-\omega_n) - p(E)\Omega_j(\omega_n)] \quad (\text{D11})$$

which is equivalent to (D7) and (D6) once one takes $N_+/N_n = (1 + \tanh(\beta_E \omega_n/2))/2$.